Transactions on Environment, Energy and Earth Sciences
ISSN: 2960-1924, eISSN: 2960-2300 | Volume 5
EMCEME 2025

Exploration of different biomasses as graphite cathode precursors for dual-ion batteries

Hongyi Luo *

School of Energy and Chemical Engineering, Xiamen University, Selangor, Malaysia

* Corresponding Author Email: EGE2309329@xmu.edu.my

Abstract. Following lithium batteries, dual-ion batteries have attracted attention for their inherent benefits of affordability, elevated voltage, and environmental sustainability. As a key component of such batteries, the performance characterization of graphite cathode is crucial for their cycle stability. In order to minimize the barrier to anion embedding in the graphite cathode, the electrode material needs to be characterized by a high degree of graphitization as well as a suitable layer spacing. Therefore, this paper compares the properties of five biomass materials used for the fabrication of carbon electrodes, namely coconut shell, ginger root, microcrystalline cellulose, kraft lignin and bamboo, after graphitization from the data point of view of ID/IG values as well as (002) facet spacing. In these five data sets, the best graphitization was in coconut shell but the best layer spacing was in ginger root. And in the comparison of the main components of biomass, cellulose performed better than lignin overall after graphitization. Further, this paper makes conjectures about better results with high cellulose content of general biomass precursors and measures to dissolve feedstock lignin and hemicellulose. In addition, this paper recommends the graphitization of biomass using an iron-cobalt catalyst and carbonization heating conditions above 1300°C.

Keywords: Dual-ion battery; graphite cathode; biomass.

1. Introduction

Lithium batteries are one of the most widely used batteries on the market today. However, as the demand for battery energy density increases and lithium battery safety accidents occur frequently, people are beginning to explore batteries more suitable for energy storage. Therefore, "dual-ion batteries" have gradually come into the research field. This battery concept first appeared in 1938 in Rudolph and Hoffman's research on insertable graphite batteries, but was only formalized in 2012 by Placke et al. After a long period of development, in 2023, Yuan et al. proposed a new type of ion battery containing an innovative electrolyte that could enhance the specific discharge capacity to more than 350 $mAh \cdot g^{-1}$. Unlike traditional lithium batteries, dual-ion batteries work with anions and cations in their electrolyte that are jointly involved in the conversion of electrical energy. For this particularity, dual-ion batteries require electrodes that can accommodate the embedding of ions, and carbon materials containing a graphene-like structure can fulfill this requirement. Pure graphene is an advanced aromatic monatomic layer of thick carbon atoms with good theoretical surface area (2630 m^2/g), electrical conductivity (2000 S/cm) and intrinsic electron mobility (2-2.5×10^5 $cm^2 \cdot v^{-1} \cdot s^{-1}$) [1]. Its precursor, graphite, has a third-dimensional structure that allows for spacing and weak interactions between layers or between graphite and substrate, which permits the embedding of ions as well as the conduction of electrons. However, existing studies have shown that pure graphene cannot directly replace the current carbon-based commercial electrode materials in batteries due to factors such as low battery cycling stability [2].

Based on this, coupled with the richness and diversity of biomass resources on earth, graphite electrodes made of biochar possessing non-pure graphite structure have gradually gained significance for dual-ion batteries. In Southeast Asia, explorations are emerging on the conversion of biomass with regional specialties, such as palm leaves and coconut shells, into carbon materials, including graphite electrodes. And the synthesis of such electrode carbon materials involves the processing of biogenic carbon. According to the reference, biogenic carbon is a hard carbon material consisting of

a disordered arrangement of graphite microcrystals strongly crosslinked by sp^2 hybridized carbon atoms (about 71%) and sp^3 hybridized carbon atoms (about 29%). The small and disordered graphite microcrystals (<20 Å) of hard carbon lead to an inability to integrate the properties of the parts, and also to a low specific surface area and conductivity, which hampers the application of biochar. Therefore, hard carbon needs to be transformed into a carbon material possessing a short-range ordered graphitic structure by undergoing structural reorganization at elevated temperatures [3]. However, the properties of carbon materials generated from different biomass precursors after processing will be different due to the presence of different compositions, structures, processing methods and other factors. In this paper, suitable conditions of bio-carbon precursors for the cathode of dual-ion batteries will be analyzed and deduced by comparing the differences in the properties of these carbon materials.

2. Graphite Cathode Synthesis Overview

2.1. Structure and mechanism of dual-ion battery with graphite cathode

The battery takes the following structure in Fig. 1 [4]. From negative to positive, the order of the components is: negative case, spring, spacer, anode, separator, cathode and positive case. Among them, the anode can be made of carbonaceous, metallic, organic and recent emerging materials such as MOFs, COFs, MXenes, etc., while the cathode is mostly made of graphite. Meanwhile, the electrolyte is often a mixed solvent system with alkyl carbonates such as ethylene carbonate (EC), propylene carbonate (PC) or low-viscosity diethyl carbonate (DEC) of $LiPF_6$ [5]. As for separators, they are often made of polyene microporous membranes such as PE, PP or their composite membranes, especially PP/PE/PP triple separators, which have a low melting point, a high puncture strength, and play a role in thermal insurance [6].

Unlike conventional batteries, the anions and cations in a dual-ion battery are both involved in energy conversion. Taking the example of a dual-ion battery with lithium anode, graphite cathode, and $LiPF_6$ electrolyte, when charging, the cation Li^+ in the electrolyte moves to the anode and combines with the electrons to form a lithium monomer, which is deposited on the surface of the negative electrode ($xLi^+ + xe^- \rightarrow xLi$). At the same time the anion PF_6^- moves toward the cathode to be embedded in the graphite interlayer ($xPF_6^- + C_n \rightarrow C_n(PF_6)x + xe^-$). Therefore, the concentration of electrolytes decreases. When discharged, the anode lithium loses electrons to become lithium ions, which move away from the anode into the electrolyte ($xLi \rightarrow xLi^+ + xe^-$). While the PF_6^- particle of the cathode is de-embedded from the graphite and moves away from the graphite cathode ($C_n(PF_6)_x + xe^- \rightarrow xPF_6^- + C_n$). In tandem, the concentration of the electrolyte recovers [7].

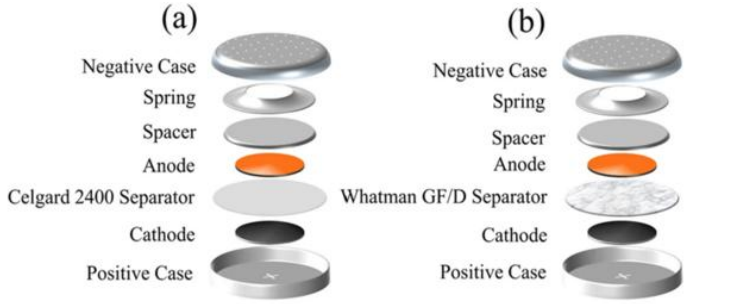

The assembly method of the full coin cell. **a** Separator uses polyethylene/polypropylene (PE/PP) Celgard 2400. **b** Separator uses fiberglass Whatman GF/D

Fig 1. Structure of dual-ion battery [4].

2.2. Performance and synthesis of biomass-derived graphite

2.2.1. Precursor selection and analysis criteria

According to the relevant references, to improve the cycling stability of dual-ion batteries, from the electrode material aspect, it needs to need to improve the degree of graphitization, layer spacing, pore

conditions, etc. [8, 9]. Therefore, this paper will focus on the ID/IG values of the fabricated graphite materials as well as the layer spacing d. In the experimental data, the ID/IG value reflects the degree of carbon structural ordering of the material. ID and IG represent the peak intensities of the disordered carbon peak (at 1350 cm^{-1}) and the graphitized carbon peak (at 1580 cm^{-1}), respectively. The smaller the ID/IG value, the greater the graphite structure share, the higher the degree of ordering and the more stable and electronically efficient the anion embedding. In addition, this paper will explore the value of the layer spacing d_{002} in terms of the (002) crystal plane. The common graphite layer spacing is about 3.34 Å, while the anion PF_6^- ion radius, which is common in the electrolyte, is 4.36 Å. So at PF_6^- insertion, the particles have to overcome a large resistance. Therefore, within a certain range, the larger d_{002} is, the easier the ion embedding is and the weaker the graphite volume fatigues and damages the graphite structure will suffer due to the repeated expansion of graphite volume in the cycle [10]. However, since the layer spacing of graphite is too much directly related to the degree of ordering, it is difficult to satisfy both metrics at the same time. In this paper, ID/IG value is prioritized and other properties are also taken into account.

According to Krishnan, S. G., the current main methods of graphitization of biomass and related parameters are shown in **Table 1** [11]. In this paper, coconut shell, ginger root, microcrystalline cellulose, kraft lignin and bamboo were selected as precursors (with '*' ahead in the table) for analysis due to their representative special performances.

Table 1. Summary of biomass catalytic graphistization (Note: 'n.a' = not available) [11].

Carbon source	Catalyst	Reaction conditions		Surface area, m^2/g	ID/IG	Crystallite size, nm		Interlayer distance, nm
		Temperature, ℃	Time, h			L_a	L_c	
*Ginger root	Pt/Al	800	1	320.67	1.10	n.a	n.a	0.363
Moringa oleifera stem	$FeCl_3$; $ZnCl_2$	800	2	2250	1.08	n.a	n.a	n.a
Sawdust	Ni-Mo	750	2	1366.54	1.05	n.a	n.a	n.a
*Bamboo	Fe-Co	850	1	317	1.78	n.a	n.a	0.34
*Coconut shell	K_2CO_3	900	2	1506.2	0.088	n.a	n.a	0.346
Porphyra	$Ni(NO_3)_2$	800	1	811.2	4.17	n.a	n.a	0.345
Microcrystalline cellulose	$NiCl_2$	1400	3	n.a	0.50	n.a	n.a	0.340
Mangosteen peel	$CoCl_2$	800	2	1168.0	1.26	n.a	n.a	0.340
*Kraft lignin	Cu, Ni, Mo, Fe	1000	1	Fe-108	Fe-1.29	14.9	n.a	Fe>Ni>Mo>Cu
Sucrose	$Fe(NO_3)_3$	700	1	198.0	~1.0	n.a	n.a	0.337
Cellulose	$Fe(NO_3)_3$	850	0.5	185.23	1.65	n.a	n.a	n.a
Softwood sawdust	$Fe(NO_3)_3$	800	1	220.0	n.a	n.a	n.a	n.a
Wood sawdust	$Fe(NO_3)_3$	850	1	n.a	n.a	35.8	56.1	0.337
Microcrystalline cellulose	$Fe(NO_3)_3$	1800	1	n.a	~0.1	7.2	6.4	0.204
*Microcrystalline cellulose	$Ca(NO_3)_2$	1400	1	n.a	0.59	>6.0	7.69	0.345
Microcrystalline cellulose	$Ca(NO_3)_2$	1400	1	n.a	n.a	n.a	7.69	0.341
Lignin	$Ca(NO_3)_2$	1400	1	n.a	n.a	n.a	17.41	0.340

2.2.2. Coconut shell

The best graphitized carbon precursor in this table is coconut shell, with an astonishing ID/IG of 0.088, which is much lower than the other carbon precursor substances, suggesting that the composition of the material or means of processing in this group has advantages. The primary constituents of biomass materials are cellulose, hemicellulose, and lignin. While coconut shell is mainly composed of cellulose (30.22%), hemicellulose (10.13%), lignin (47.13%), extractives (4.51%), water (5.6%), and ash (2.36%). Upon comparison, it was found that the coconut shell composition was high in lignin and low in cellulose and ash. As for the process, coconut shells were first pulverized to less than 100 μm in size. They were then heated at 400 °C in nitrogen gas flow for 3 h and cooled naturally to produce biochar. Next, the biochar powder was mixed with potassium carbonate at a weight ratio of 1:2. Then it was heated to 900°C in nitrogen gas flow and held for 2 hours. After cooling naturally, the sample was rinsed with dilute hydrochloric acid and then deionized water to achieve a neutral pH. The final product was got after drying at 60 °C for 12 h. During the process, the potassium carbonate catalyst allowed graphite microcrystals to be released from crosslinked sp^3 carbon atoms in the hard carbon phase of biochar at 900 °C, which were then recrystallized to form three-dimensional porous graphene-like sheets (3DPGLS). The 3DPGLS generated consists of 3 to 4 layers of graphene, which has a interlayer distance of 0.346 nm. When tested in the capacitor, this electrode material can have a capacitance retention rate of 85.1% after 5000 cycles at a current density of 0.1 A/g, showing its good potential in cycling stability. Moreover, similar results were obtained using walnut, pistachio, apricot and hazelnut shells of similar composition. This further supports the superiority of the combination of the material selection and synthesis methods [12].

2.2.3. Ginger root

The precursor with largest interlayer spacing in this table is ginger root, up to 0.363 nm. The ginger root used in the experiment had a water content of 79 g per 100 g and contained less than 2 g of insoluble fiber [13], which was mainly cellulose (70.05 wt%), hemicellulose (26.45 wt%) and lignin (3.5 wt%) [14]. It also contains small amounts of minerals such as K, Mg, P, Ca, and Na at milligram level.

In this study, ginger root was firstly peeled and sliced. To eliminate contaminants, it was then washed by deionized water. After that, it was dried completely at 240 °C overnight. The pretreated ginger root sample was then heated at 800°C in argon flow for 1 h. Subsequently, the product was mashed and processed into fine powders. Finally, the impurities and large particles are further removed by centrifugation and washing by ethanol and deionized water.

During pyrolysis, a porous structure is formed because of the decomposition of precursor materials with the presence of minerals that act as porosity agents, thereby increasing the surface area. Several layers of graphene-like carbon nanosheets were finally generated with an ID/IG value of 1.1. When this ginger root-derived carbon material was used as a capacitor electrode, it maintained 93.3% capacitance after 3500 charge/discharge cycles [15].

2.2.4. Microcrystalline cellulose

Cellulose consists of a long chain of D-glucose molecules with only sp^3 carbon. During cellulose pyrolysis, the sp^3 carbon undergoes several complex and orderly chemical rearrangements to sp^2 carbon, forming an aromatic ring. The study of B'eguerie T mentions that pyrolysis of calcium-impregnated microcrystalline cellulose at 1800 °C under nitrogen can produce graphitized carbon. In the study, 40 g of cellulose was soaked at first in 200 ml of deionized water with calcium nitrate dissolved in it for 6 hours with stirring. The impregnated cellulose was then filtered and dried and then pyrolyzed at 800 °C for 1 hour. The biochar got was then heated to 1800°C under nitrogen at an elevated rate of 2°C per minute and maintained for 1h to obtain the final product. The study also compares the catalytic effect of different concentrations of calcium nitrate, with the best performance at a concentration of 3.83 wt%. Its graphite layer spacing was 0.345 nm and the local ID/IG value

could reach 0.59. This is similar to commercial graphite (layer spacing: 0.338 nm, ID/IG: 0.23). In contrast, the spectrum of unimpregnated cellulosic biochar has broad and intense D and G bands and has an ID/IG value of 1.34 [16]. Catalysts can significantly improve the quality of graphite.

2.2.5. Kraft lignin

In Yan's research, kraft lignin, a byproduct of the wood pulping industry, was used as a carbon precursor. Due to the use of sodium sulfide as one of the pulping reagents, the structure of kraft lignin contains sulfur impurities. Meanwhile, this study also analyzed the effect of transition metals Cu, Ni, Mo and Fe on the catalytic graphitization of kraft lignin.

As an example, the experimental procedure for the iron catalyst is as follows: First, kraft lignin was added to tetrahydrofuran and stirred for 2 hours. Meanwhile, ferric nitrate hydrate was added to deionized water and stirred until completely dissolved. Then, the ferric nitrate solution was added dropwise to the kraft lignin solution and agitated for 2 h. The solution was then added to the kraft lignin solution. The mixture was kept at room temperature for 24 hours and then dried at 110°C for another 24 hours. After that, 15 g of the product got was heated to 1000 °C in an argon atmosphere and held for 1 h. The final product was then obtained after cooling to room temperature.

After characterization tests, the ID/IG values of carbon materials at the four catalysts were Fe (1.29) < Ni (1.39) < Mo (1.46) < Cu (1.50). It is shown that the graphitization activity of the catalyst increases in the order of Cu < Mo < Ni < Fe. In addition, although the study does not explicitly list graphite layer spacing values for each group, the overall effect is still in line with the ranking [17].

Compared with other transition metal catalysts, the iron-based catalysts showed their superiority. The rationale for this, the "carbon dissolution-precipitation" mechanism, is clearly presented in Hunter’s study: Fe nanoparticles are gradually formed at around 700°C. The contact between Fe and C causes amorphous carbon to dissolve on Fe nanoparticles and precipitate into ordered graphitic carbon [18]. However, the study also points out that more catalyst does not always mean better result. Principle speaking, excessive amounts of iron will lead to an increase in its particle density, which makes it easier to aggregate as the particles migrate. This results in larger particle size and reduces catalytic activity. Besides, according to the data, the layer spacing of the material decreases with increasing catalyst dosage, which is not good for anion embedding.

2.2.6. Bamboo

The effect of a single catalyst did not reach the optimal state of catalysis. The study of Rusch proposed a method of co-catalysis by multiphase catalysts. Besides, the study explored the effect of heating temperature.

For composition, Bamboo mainly possesses lignin (25.5%), cellulose (40-60%), ash (2.2%), and extractive components (5.9%) [19]. The contents of cellulose, hemicellulose and lignin in bamboo are similar to wood lignocellulose, but its extractives, ash and silica contents are higher.

Taking Fe-Co catalyst as an example, the study at first dispersed the bamboo powder in a mixture containing iron nitrite (0.5mmol), cobalt nitrite (0.5mmol) and deionized water (10mL). After shaken for 24 h, the products were dried to obtain preliminary samples. As for other groups, relevant measures were taken to make the variables minimal and simple. Then, 2 g of the sample from each group was heated to the set temperatures and held for 1 h. The product was washed with excess hydrochloric acid, further washed with deionized water and dried to obtain the final product.

According to the data, the ID/IG values of products are the smallest under iron-cobalt co-catalysis at 850 °C: Fe-Co(1.78) < Fe-Ni(1.97) < Fe(3.05) < Fe-Ni(3.05) < Co(3.34) < Ni(3.37) < none(4.08). Besides, the layer spacing can be deduced from the degree of graphitization according to relevant equation: Fe-Co(0.3403nm) < Co(0.3407nm) < Fe(0.3423nm) < Ni(0.3424nm) < Fe-Ni(0.3426nm). Although the layer spacing of the group with Fe-Co catalyst was slightly smaller than the other catalysts, its ID/IG value was more significantly smaller than the other groups. Therefore, it is considered to perform the best. In addition, the research has also studied in detail the graphitization

effect of bamboo at different temperatures. Although the study pointed that the carbon material's specific surface area reaches its peak at 850°C, which refers to the best pore conditions, the ID/IG values of the samples between 850°C and 1300°C still keep decreasing with increasing temperature [20], which can probably provide more stable cycling conditions for the battery. Therefore, for biogenic carbon precursors of similar composition, the graphitization temperature is preferably maintained at 1300°C or above.

2.2.7. Overall analysis

In summary, in order to obtain batteries with better cycling stability, it is necessary that the material preferentially has a low ID/IG value and is also characterized by a large graphite layer spacing. On the one hand, this requires suitable biomass precursors. According to the above five sets of data, cellulose has better properties than lignin after graphitization as far as a single component is concerned. This may be related to the fact that cellulose possesses a more regular structure, which is shown in **Fig. 2** below for cellulose and lignin [21]. For general carbon precursors, performance can be enhanced by removing the lignin component. Whereas, according to the literature, combined NaOH bleaching treatment can further degrade the complex lignocellulosic structure, causing hemicellulose and lignin to disintegrate. This treatment also reveals more porosity and expands the accessible surface area for hidden cellulose [22]. However, biomass precursor samples with high lignin content, such as coconut shells, showed anomalous graphitization with better overall performance, which may be due to the interactions between the components as well as the processing conditions, but the exact principle is not clear. On the other hand, methods for synthesizing graphite structures need to be optimized. For general biomass samples, graphitized carbon needs to be obtained by pretreatment, preliminary carbonization, catalyst doping, high temperature sintering graphitization, acid washing and drying. It is predicted that among them, the use of iron-cobalt dual catalyst catalyzed and processed at 1300°C and above is relatively effective.

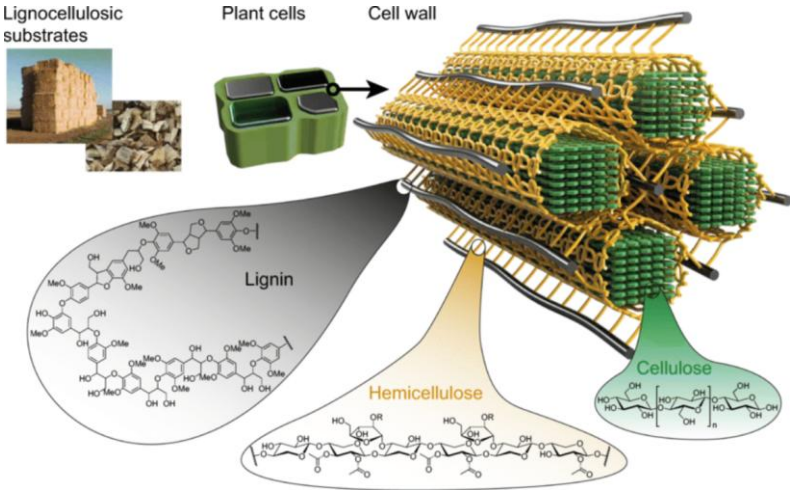

Fig 2. Structure of each component in lignocellulose [21].

3. Conclusion

In conclusion, dual-ion batteries are gradually coming into the research field due to the special joint participation of anions and cations in energy storage. However, the cycling stability of dual-ion batteries needs to be improved, which is partly caused by the barrier of anion embedded in graphite. This is explored in this paper and it is found that reducing the ID/IG value of the material is the fundamental solution, while increasing the layer spacing and improving other characterization properties are also important. Among the given biomass-derived graphite methods, five characteristic samples of coconut, ginger root, microcrystalline cellulose, kraft lignin, and bamboo were selected for the study and comparison in this paper. As far as the single component of biomass is concerned, cellulose was found to have better ID/IG values and layer spacing data than lignin, speculating that this may be due to the highly regular structure of cellulose. However, for the remaining three groups

of naturally occurring biomass, coconut shell with low cellulose content instead performs better. This situation may be related to the interaction between multiple components and the differences in graphitization processes. In general, to improve graphite performance, lignin could be chemically removed. As for the processing flow, this paper suggests that graphitization of carbon precursors can be carried out with the use of Fe-Co catalysts and at temperatures above 1300°C to improve the graphite properties.

References

[1] Azam, M. A., Zulkapli, N. N., Dorah, N., Seman, R. N. a. R., Ani, M. H., Sirat, M. S., Ismail, E., Fauzi, F. B., Mohamed, M. A., & Majlis, B. Y. Review—Critical Considerations of High quality graphene synthesized by Plasma-Enhanced Chemical vapor deposition for electronic and energy storage Devices. ECS Journal of Solid State Science and Technology, 2017, 6(6): M3035–M3048.

[2] Zhu J, Duan R, Zhang S, et al. The application of graphene in lithium ion battery electrode materials. SpringerPlus, 2014, 3(1): 585.

[3] Xia J, Zhang N, Chong S, et al. Three-dimensional porous graphene-like sheets synthesized from biocarbon via low-temperature graphitization for a supercapacitor. Green Chemistry, 2018, 20(3): 694-700.

[4] Xue Z, Guan D, Zeng J, et al. Research on the assembly process of full coin cells: key factors affecting data reliability. Ionics, 2023, 29(12): 5285-5293.

[5] Wang, Q., Sun, J., Yao, X., & Chen, C. Thermal stability of $LiPF_6$/EC+DEC electrolyte with charged electrodes for lithium ion batteries. Thermochimica Acta, 2005, 437(1–2): 12–16.

[6] Li, Y., Pu, H., & Wei, Y. Polypropylene/polyethylene multilayer separators with enhanced thermal stability for lithium-ion battery via multilayer coextrusion. Electrochimica Acta, 2018, 264: 140–149.

[7] Wu H, Luo S, Wang H, et al. A Review of Anode Materials for Dual-Ion Batteries. Nano-Micro Letters, 2024, 16(1): 252.

[8] Shen Y, Zhang M, Yan D, et al. Soft Carbon as Cathode with High Rate Performance for Dual-Ion Batteries via Fast PF_6^- Intercalation Improved by Surface Effect. ChemSusChem, 2023, 16(17): e202300493.

[9] Cameán I, Lobato B, Omnée R, et al. Optimization of Textural and Structural Properties of Carbon Materials for Sodium Dual-Ion Battery Electrodes. Molecules, 2025, 30(11): 2439.

[10] Kumar S, Bhauriyal P, Pathak B. Computational Insights into the Working Mechanism of the $LiPF_6$–Graphite Dual-Ion Battery. The Journal of Physical Chemistry C, 2019, 123(39): 23863-23871.

[11] Krishnan S G, White C E, Zeng K, et al. Recent developments on multi- versus single-metallic catalytic graphitisation of biocarbon: A review. Fuel, 2025, 396: 135330.

[12] Xia J, Zhang N, Chong S, et al. Three-dimensional porous graphene-like sheets synthesized from biocarbon via low-temperature graphitization for a supercapacitor. Green Chemistry, 2017, 20(3): 694-700.

[13] U.S. Department of Agriculture, Agricultural Research Service. FoodData Central: Nutrients for Food ID 169231. 2019. https://fdc.nal.usda.gov/food-details/169231/nutrients

[14] Eyupoglu S. Characterization of New Cellulosic Fibers Obtained from Zingiber Officinale. Journal of Natural Fibers, 2020, 19(4): 1287-1296.

[15] Gopalakrishnan A, Kong C Y, Badhulika S. Scalable, large-area synthesis of heteroatom-doped few-layer graphene-like microporous carbon nanosheets from biomass for high-capacitance supercapacitors. New Journal of Chemistry, 2018, 43(3): 1186-1194.

[16] Béguerie T, Weiss-Hortala E, Nzihou A. Calcium as an innovative and effective catalyst for the synthesis of graphene-like materials from cellulose. Scientific Reports, 2022, 12(1): 21492.

[17] Yan Q, Li J, Zhang X, et al. Catalytic graphitization of kraft lignin to graphene-based structures with four different transitional metals. Journal of Nanoparticle Research, 2018, 20(9): 223.

[18] Hunter, R. D., Ramírez-Rico, J., & Schnepp, Z. Iron-catalyzed graphitization for the synthesis of nanostructured graphitic carbons. Journal of Materials Chemistry A, 2022, 10(9): 4489–4516.

[19] Rusch F, Wastowski A D, De Lira T S, et al. Description of the component properties of species of bamboo: a review. Biomass Conversion and Biorefinery, 2021, 13(3): 2487-2495.

[20] Xia S, Yang H, Lu W, et al. Fe–Co based synergistic catalytic graphitization of biomass: Influence of the catalyst type and the pyrolytic temperature. Energy, 2022, 239: 122262.

[21] Brethauer, S., Shahab, R. L., & Studer, M. H. Impacts of biofilms on the conversion of cellulose. Applied Microbiology and Biotechnology, 2020, 104(12): 5201–5212.

[22] Bichang'a D O, Oladele I O, Alabi O O, et al. Comparative property investigation of raw and treated coconut shell biomass for potential polymer composite application. Heliyon, 2024, 10(23): e40704.